Reliability analysis of cold-formed steel beams susceptible to distortional buckling using numerical analysis data incorporated into the professional factor variable

Márcio M. da Silva[1], Washington B. Vieira[2], André L. R. Brandão[2], Marcílio S. R. Freitas[1]

[1]*Programa de Pós-Graduação em Engenharia Civil, Universidade Federal de Ouro Preto, Escola de Minas, Campus Morro do Cruzeiro, 35400-000, Ouro Preto, Minas Gerais, Brasil.*
marcio.maciel@aluno.ufop.edu.br, marcilio@ufop.edu.br
[2]*Instituto de Engenharias Integradas, Universidade Federal de Itajubá. Campus Theodomiro Carneiro Santiago, Rua Irmã Ivone Drumond, 200, Distrito Industrial, 35903-087, Itabira, Minas Gerais, Brasil.*
vieira@unifei.edu.br, andreriqueira@unifei.edu.br

Abstract. In cold-formed steel (CFS) beams subjected to simple bending with restriction to lateral-torsional buckling and without restriction on the compressed flange, distortional buckling can be the predominant failure mode. This work aims to develop a study on the distortional instability mode in CFS lipped C-section subject to simple bending by numerical analysis using ABAQUS finite element software and CUFSM, a finite strip method software. The Matlab software was used to automate the modeling so that a range of numerical simulations with material and geometric nonlinearity was performed and validated with experimental results from the literature. A reliability analysis with the FORM method was performed using load combinations according to the calibration parameters of AISI-LRFD and AISI-LSD to obtain the reliability index (β) and probability of failure (P_F). From these results, it was observed a good achievement between the reliability indexes of the models and the established target index of $\beta_o = 2.50$, a reference for the calibration of the AISI-LRFD.

Keywords: Reliability analysis; Numerical analysis; Cold-formed steel beams; Distortional buckling; DSM.

1 Introduction

Cold-formed steel (CFS) profiles are used in various fields of civil construction, such as buildings, roofs or sheds, in which they are susceptible to different types of loads. These profiles are made of thin plates and are light profiles with versatility of cross sections and exhibiting a high slenderness. It is possible to observe problems of instabilities, excessive deformations and even collapse, however, when well used, it has high structural efficiency.

The failure in CFS beams can be initiated by one of the three instability modes: local buckling, distortional buckling or lateral-torsional buckling (LTB). LTB restrained beams without restraints on the compression flange, distortional buckling may be the predominant failure mode. In this mode, the flange and lip rotate around the web, with some rotational resistance set by the web. Generally occurring at shorter wavelengths than LTB, but longer wavelengths than local buckling [1]. The distortional buckling mode is a type of instability with few experimental data available in the literature, compared to other buckling modes.

The article tried to analyze the distortional instability mode in CFS lipped C-section in simple bending by the finite element method (FEM) using the ABAQUS software [2]. Furthermore, an analytical analysis was performed with the application of the Direct Strength Method (DSM) with the aid of the finite strip method (FSM), using the CUFSM software (Schafer and Ádàny [3]). The results were validated with experimental data from several authors [4, 5, 6], verifying the critical moments of buckling and their respective collapse modes.

In order to verify the safety taking into account uncertainties, the First Order Reliability Method (FORM) was used [7]. The load combinations were determined according to the calibration parameters of AISI-LRFD and AISI-LSD to obtain the reliability index (β) and probability of failure (P_F), with the target $\beta_o = 2.50$, a reference

for the calibration of the AISI-LRFD (AISI S100 standard [8]).

2 Methods: buckling analysis

2.1 Direct strength method

The Direct Strength Method (DSM) is included in annex C of NBR 14762 [9] and in the AISI S100 standard [8], providing calculations to obtain the resistance to simple bending, due to local buckling, distortional buckling or LTB. For the application of the proposed formulations it is necessary to analyze the elastic stability of the bar, so the CUFSM software [3] that uses the FSM was adopted.

The calculation of the CFS lipped C-section properties was done using NBR 6355[10]. In summary, the characteristic value of the bending moment resistance (M_{Rk}) is defined as the smallest among the calculated values LBT (M_{Re}), local buckling (M_{Rl}) and distortional buckling (M_{Rdist}).

2.2 Finite element modelling

The finite element modeling developed in ABAQUS[2] was standardized with simulations of individual CFS lipped C-section beams, considering the material and geometric nonlinearity. The first modeling step consisted of defining the geometric model, so that the physical problem was adequately represented in the computer simulation. Initially, it was verified the behavior of the CFS, from numerical simulations, of several works available in the literature [4, 11, 12, 13], whose authors obtained good results in their analyses. Given the above circumstances, numerical modeling was defined as three-dimensional, in the form of a shell, of the deformable type. A perfect elasto-plastic constitutive model was adopted, in which the residual stresses were not considered.

Boundary conditions imposed on the model must respect the actual behavior of the structure. In order to avoid displacement of rigid body, displacement in the longitudinal direction has been restricted. At the end nodes of lipped C-section, displacements in the *x*- and *y*-directions were restricted, and the rotation in the *z*-direction, in the region of the coupling of the plate with the profile, a restriction was imposed on the displacement of the *x*-direction and the rotation of the *z*-direction, in order to avoid the LTB.

Loading was applied to the element as a linear disturbance of the buckle type and the solution is obtained by the subspace iteration method [14]. The result of this analysis are the eigenvectors and eigenvalues that represent respectively the mode and the critical load of buckling. The type of loading adopted was a concentrated unitary force, in the shear center of the profile, however, it is displaced from the face of the profile web, therefore, it was necessary to insert plates for the application of the load, such as shown in fig.1.

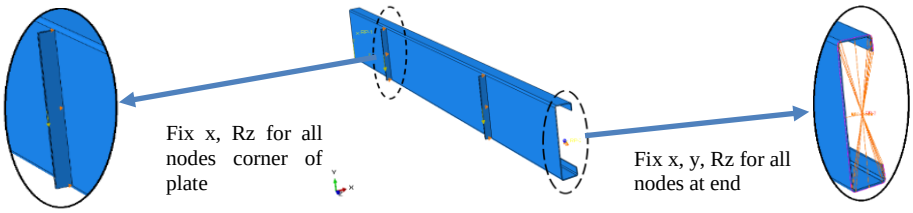

Figure 1. Profile modeling with plate insertion and boundary conditions

Two possibilities were evaluated in 14 simulations of different lipped C-section, being the numerical bending moment resistance (M_{FEM}) from the simulation with the connected plate (CP), and the numerical bending moment resistance from the simulation with the plate being part of the profile (PP). It can be seen that the PP modeling presented a better approximation with the experimental bending moment resistance (M_{Test}), adopting this modeling for the other profiles. The thickness of the plate used initially was 5 mm, and subsequently thicknesses of 10 mm, 15 mm and 20 mm were adopted to assess the interference of the plate in the bending moment resistance. There was a insignificant influence on the increase in thickness from 5 mm to 20 mm, as shown in Tab.1:

Table 1. Plate thickness influence

Thickness (mm)	M_{FEM} (kN.m)
5	5.6848
10	5.6850
15	5.6852
20	5.6853

The subsequent nonlinear analysis approached the initial geometric imperfections as a function of the eigenvector obtained from the elastic buckling analysis. The imperfections magnitude influence the results of the nonlinear analysis, thus, a range of imperfection values introduced in the modeling were verified with magnitudes equal to: profile thickness (Schafer and Pekoz [12]), *L*/750 being *L* equal to the unlocked length between the load application points (Yao and Guo [4]) and F/50 where F is equal to the width of the flange (Pastor *et al.* [13]).

Aiming at computational efficiency, reduced numerical integration is attractive since the number of integration points is reduced from four to one. It was chosen to use the finite element called S4R having six degrees of freedom at each node [2].

The mesh discretization in finite elements was defined by the mesh objectivity, relating the computational effort time and the precision of the results. Fig.2a is a graphical representation between the bending capacity and the rotation angle, being captured at the node located longitudinally at ¼ of the profile length (load application region) and transversely at its neutral axis. Fig. 2b relates the bending capacity and the vertical displacement being obtained in the node located longitudinally in ½ of the profile length and transversally in the center of the upper flange, both with meshes of 5x5 mm, 10x10 mm, 30x30 mm and 50x50 mm. Tab.2 represents the processing time and precision of the bending moment resistance. The 10x10 mm mesh was then adopted for other profiles. The results called Test and FEM were obtained from the literature (Yao and Guo [4]).

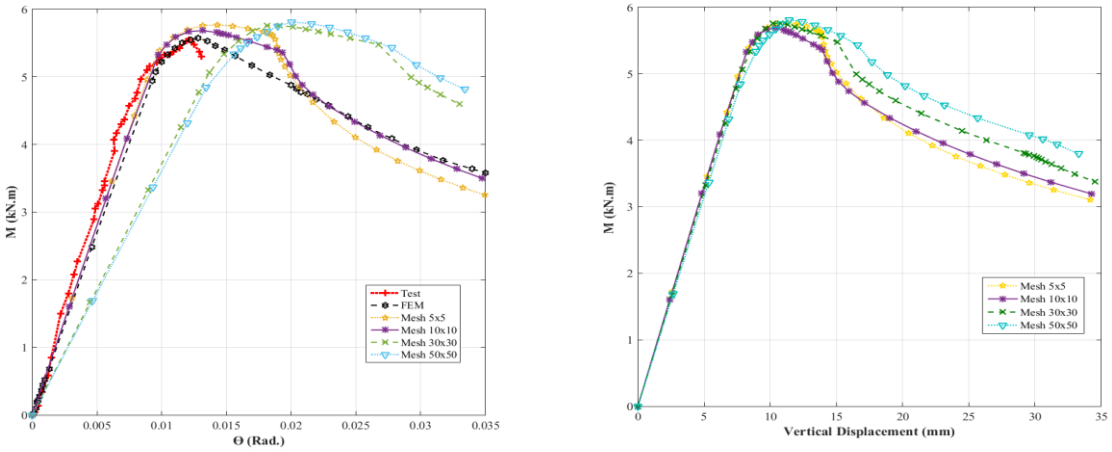

(a) (b)

Figure 2. (a) Moment-rotation curve; (b) Moment-vertical displacement curve

Table 2. Mesh objectivity

Mesh (mm)	M_{FEM} (kN.m)	$M_{Test.}/M_{FEM.}$	Processing time
5x5	5.7676	0.9623	30'13"
10x10	5.6847	0.9763	8'26"
30x30	5.7596	0.9636	1'46"
50x50	5.8111	0.9551	1'32"

Nonlinear analysis was performed using the modified Riks method (arc-length method). After processing, the eigenvector of the analysis is multiplied by a scalar that represents the maximum geometric imperfection in

the part, obtaining the resistance moment of the bar and its collapse mode. A high similarity between the collapse modes can be observed, as shown in fig.3.

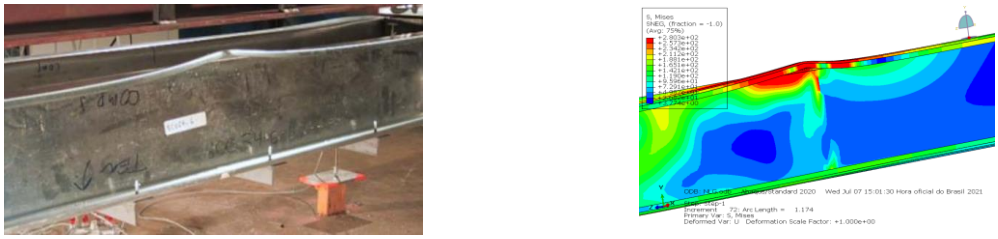

(a) (b)

Figure 3. Collapse mode: (a) Test (Yu and Schafer [5]); (b) Numerical simulation, FEM

After defining all steps of numerical modeling, analysis automation was implemented by the MATLAB software, standardizing the subsequent simulations from a base model, changing the variables according to each test, such as geometric dimensions of the section and material properties, generating the models in ABAQUS from the modified scripts.

3 Reliability analysis: First-Order Reliability Method (FORM)

The structural reliability theory is based on the probabilistic modeling of uncertainties associated with resistance and stresses, providing methods for determining the probability of structures not meeting the performance criteria. In the present article, the First-Order Reliability Method (FORM) was adopted, approaching the performance function iteratively, until there is convergence to the design point, located at the minimum distance from the origin to the performance function [15].

Initially, the performance or limit state function G(X) is defined, where X corresponds to its random variables, X_1, X_2, X_3,..., X_n, involving resistance (R) and loading effects (S) variables. Considering all the variables as independent, there is the generalized eq.(1), where the effects of resistance and loading effects are implicit (Melchers and Beck [7]).

$$f_x(x) = \prod_{i=1}^{n} f_{X_i}(x_i) = f_{x_1}(x_1).f_{x_2}(x_2).f_{x_3}(x_3)\ldots \tag{1}$$

The random variables used in the reliability analysis related to structural resistance are generally given as a function of material (M), fabrication (F) and professional factor (P) properties and, in this case, the structural requirements arising from the Dead Load (D) and Live Load (L). One can write the performance function according to eq.(2) (Hsiao [16]).

$$G(.) = R_n\, M.F.P - c.(D+L)\,. \tag{2}$$

ABNT NBR 14762[9] presents statistical parameters for the material factor and fabrication factor random variables and for Dead Load and Live Load, those proposed by Ellingwood et al. [17] and Hsiao [16]. The variable professional factor (P), or model error, arising from modeling uncertainties until the element strength was obtained, was established according to the formulations that relate the experimental data for validation and calibration of numerical simulations, suggested in the Technical Memoranda of SSRC[18], relating the experimental moment (M_{Test}) with the moment from the numerical simulation (M_{FEM}) and the moment from the DSM (M_{DSM}), for all tests, as shown in equations (3) and (4):

$$P_1 = \frac{M_{Test}}{M_{FEM}} \tag{3}$$

$$P_2 = \frac{M_{FEM}}{M_{DSM}} \tag{4}$$

According to the Technical Memoranda of SSRC[18], the mean (P_μ) and the coefficient of variation (V_P) of the professional factor variable are established as:

$$P_{\mu} = P_{1\mu} \,.\, P_{2\mu} \tag{5}$$

$$V_P = \sqrt{V_{P1}{}^2 + V_{P2}{}^2} \tag{6}$$

In the FORM method, a new design point in the reduced space (X'^{i}) is evaluated by the HLRF algorithm [19], according eq.(7), where ∇G is the gradient vector of the performance function.

$$X'^{(i+1)} = \frac{1}{|\nabla G(X'^{i})|^2}\left[\nabla G(X'^{i})^T X'^{i} - G(X'^{i})\right] \nabla G(X'^{i}) \,. \tag{7}$$

The reliability index β was obtained from eq. (8)

$$\beta = \left| X'^{(i+1)} \right| . \tag{8}$$

The probability of failure is determined from the reliability index β, by eq. (9) where Φ is the standard normal cumulative distribution function (CDF):

$$Pf = \Phi(-\beta) \,. \tag{9}$$

4 RESULTS AND DISCUSSIONS

A database consisting of 62 experimental tests in beams of lipped C-section, with the instability mode governed by distortional buckling, collected from several authors [4, 5, 6], was used to validate the proposed numerical model. The model calibration, imperfections and the type of modeling were verified, comprising a sample space of 262 simulations, arranged according to Tab. 3:

Table 3. Sample space in model calibration

Author	Method	Imperfections	Modeling	Simulations
Yao and Guo [4]	FEM	L/750	CP	14
			PP	30
		Thickness	PP	30
		F/50	PP	30
	DSM	-	-	30
Schafer and Pekoz [12]	FEM	L/750	PP	26
		Thickness	PP	26
		F/50	PP	26
	DSM	-	-	26
Javaroni [6]	FEM	L/750	PP	6
		Thickness	PP	6
		F/50	PP	6
	DSM	-	-	6

Thus, among the analyzed imperfections, the L/750 and F/50 stand out, with the PP type modeling, which led to better convergence results. Therefore, both were used in the model validation, for the subsequent simulations

of new profiles. In order to obtain the statistical parameters of the professional factor variable, the reason between the experimental moment and the bending moment resistance arising from the modeling, the Minitab 19 software was used, using the Anderson Darling method to find the distribution of probability that best fits the data. The means of $P_{F/50}$ = 1.055 and $P_{L/750}$ = 1.056 and coefficient of variation of $P_{F/50}$ = 0.1178 and $P_{L/750}$ = 0.1267 were obtained with both normal probability distribution functions.

After validating the numerical simulations, an expansion of the database was carried out, in which 108 beams of lipped C-section were added to the analysis, with 62 beams consisting of thin plates commercially used in Brazil, adopting catalogs from two companies. The other 46 beams were taken from AISI MANUAL 2013 TAB I-1 [20]. To compose the database, Tab.14 of NBR 14762[9] was adopted inversely in order to find profiles prone to distortional buckling. In the modeling, the imperfections previously validated, F/50 and L/750, were used, comprising a sample space of 216 simulations via ABAQUS and 108 simulations using the DSM, totalizing 324 simulations. Tab. 4 presents geometric dimensions of the used profiles.

Table 4. Geometric dimensions used in simulations

Geometric dimensions	Minimum dimension (mm)	Maximum Dimension (mm)
Depth	100.0	350.0
Flange	50.0	101.6 (4”)
Lip	10.0	25.0
Thichness	0.75	3.0

In order to find the statistical parameters of the professional factor variable P, the value referring to P_1 was adopted according to the previously validated simulations, and the value of P_2 was found by the new simulations, obtaining the averages of $P_{F/50}$ = 1.058 , $P_{L/750}$ = 1.104 and coefficient of variation of $P_{F/50}$ =0.135 and $P_{L/750}$ = 0.127. It is important to point out that the professional factor having an average above 1.0 represents an average reduction in the strength of the bars, causing an increase in the reliability index. Thus, the reliability index β and probability of failure were obtained, with the load factor γ = 1.1, as indicated in fig. 4.

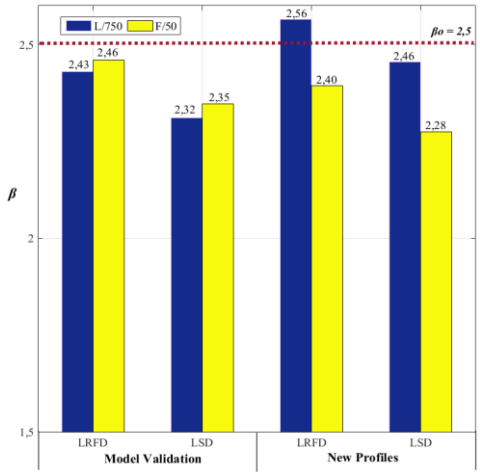

Figure 4. reliability index β for imperfections L/750 and F/50.

5 Conclusions

The modeling automation provides a fast and accurate analysis of buckling, which can minimize the time for future analysis in the academic and professional scope. Given the numerical and analytical simulations developed, which comprise a sample space of 586 simulations, it can be concluded that:

i) the bending moment resistance from FEM are sensitive to the imperfection magnitude, and for CFS lipped C-section subject to simple bending, magnitudes equal to L/750 and F/50 presented satisfactory results;

ii) the graphical representation between the bending capacity and the rotation angle shows a good

approximation between the curve from the numerical simulation with a 10 x 10 mm mesh and the Test and FEM provided by Yao and Guo [4]. Regarding the collapse modes, it can also be observed a high similarity in comparison with the actual model (Yu and Schafer [5]);

iii) when evaluating the statistical parameters of the model validation between the relation of $\frac{M_{Test}}{M_{FEM}}$, that is, analyzing P_i, a high precision between the experimental results and the numerical simulations is notable. Mean equal $\mu_{F/50} = 0.979$ and $\mu_{L/750} = 1.015$, with the coefficient of variation equal to $V_{P,F/50} = 0.098$ and $V_{P,L/750} = 0.097$, concluding that the calibrated and later validated model was necessary and satisfactory;

iv) the reliability index β found in the LRFD approach was superior to the target reliability index $\beta_o = 2.5$ for simulations with imperfections equal to L/750 in the sample space for the new profiles. However, the other analyzes found β slightly lower than $\beta_o = 2.5$.

Acknowledgements. The authors thank the UFOP (Federal University of Ouro Preto) and FAPEMIG (Fundação de Amparo à Pesquisa do Estado de Minas Gerais) for supporting the development of this research.

Authorship statement. The authors hereby confirm that they are the sole liable persons responsible for the authorship of this work, and that all material that has been herein included as part of the present paper is either the property (and authorship) of the authors, or has the permission of the owners to be included here.

References

[1] W. W. Yu, R. A. LaBoube and H. Chen "Cold-Formed Steel Design ", Fifth edition, Wiley, 2020.
[2] Hibbitt, Karlsson and Sorensen. "ABAQUS Theory Manual", USA, 2009.
[3] Schafer, B. W. and Adany, S. "Buckling analysis of cold-formed steel members using CUFSM: conventional and constrained finite strip methods". XVIII International Specialty Conference on Cold-Formed Steel Structures, 2006.
[4] X. Yao and Y. Guo. "Inelastic Test and Design Method of Cold-formed Steel Lipped Channel Members in Bending". *The Open Civil Engineering Journal, pp.*625-640, 2016.
[5] C. Yu and B.W. Schafer. "Distortional buckling of cold-formed steel members in bending". *Research Report* RP 05-1. Maryland: American Iron and Steel Institute – Committee on Specifications for the Design of Cold-Formed Steel Structural Members, 407 p, 2005.
[6] C. E. Javaroni. "Perfis de aço formados a frio submetidos à flexão: análise teórico-experimental". Tese (Doutorado em Engenharia de Estruturas), Universidade de São Paulo, 1999.
[7] R. E. Melchers and A. T. Beck "Structural Reliability Analysis and Prediction ", Third edition, Wiley, 2018.
[8] American Iron and Steel Institute AISI-S100. North American specification for the design of cold-formed steel structural members, 2016.
[9] Associação Brasileira de Normas Técnicas. NBR 14762: Dimensionamento de estruturas de aço constituídas por perfis formados a frio. Rio de Janeiro, 2010.
[10] Associação Brasileira de Normas Técnicas. NBR 6355: Perfis estruturais de aço formados a frio - Padronização. Rio de Janeiro, 2012.
[11] C. Yu and B.W. Schafer. "Finite Element Modeling of Cold-formed Steel Beams Validation and Application". XVIII International Specialty Conference on Cold-Formed Steel Structures, 2006.
[12] B. W. Schafer and T. Pekoz. "Computational modeling of cold-formed steel: characterizing geometric imperfections and residual stresses". *Journal of Constructional Steel Research*, pp. 193-210, 1998.
[13] M. M. Pastor, M. Casafont, J. Bonada and F. Roure. "Imperfection amplitudes for nonlinear analysis of open thin-walled steel cross-sections used in rack column uprights". *Thin-Walled Structures,* pp. 28-41, 2014.
[14] K. J. Bathe. "Finite Element Procedures". Prentice-Hall, New Jersey, 1996.
[15] A. Haldar and S. Mahadevan. "Probability, Reliability, and Statistical Methods in Engineering Design" . John Wiley & Sons, New York, 2000.
[16] L. E. Hsiao. Reliability Based Criteria for Cold-Formed Steel Members. Ph.D.Thesis, University of Missouri-Rolla,1989.
[17] B. R. Ellingwood, J. G. MacGregor, T. V. Galambos and C. A. Cornell, "Probability based load criteria: Load factors and load combinations." J. Struct. Div., 108(5), 978–997, 1982.
[18] R. D. Ziemian. "Technical memoranda of structural stability research council". Guide to Stability Design Criteria for Metal Structures, John Wiley & Sons, New Jersey, 2010.
[19] A. M. Hasofer and N.C. Lind, "An exact and invariant first-order reliability format". Journal of Engineering Mechanics, v. 100, p. 111-121, 1974.
[20] American Iron and Steel Institute AISI MANUAL. "Cold-Formed Steel Design", 2013.